Image charge effect and vibron-assisted processes in Coulomb blockade transport: a first principles approach

A. M. Souza,[*,†,§] I. Rungger,[†,‖] U. Schwingenschlögl,[‡] and S. Sanvito[¶]

School of Physics, CRANN and AMBER, Trinity College, Dublin 2, Ireland, PSE Division, KAUST, Thuwal 23955-6900, Saudi Arabia, and School of Physics and CRANN/AMBER, Trinity College, Dublin 2, Ireland

E-mail: souzaa@tcd.ie

Ab-initio electronic transport properties: DFT+NEGF

For the *ab-initio* quantum transport calculations, we apply the non-equilibrium Green's function (NEGF) formalism as implemented in the SMEAGOL code.[1,2] Within this approach, the retarded Green's function of the scattering region, $\mathcal{G}_{\rm D}$, is given by

$$\mathcal{G}_{\rm D}(E) = \lim_{\eta\to 0}\left[(ES_{\rm D} + i\eta) - H_{\rm D} - \Sigma_{\rm L} - \Sigma_{\rm R}\right]^{-1}, \tag{1}$$

where E is the energy, $\Sigma_{\rm L,R}$ are the self-energies of the left and right electrodes, $S_{\rm D}$ and $H_{\rm D}$ are the overlap and the Hamiltonian matrices, respectively, of the scattering region obtained from

[*]To whom correspondence should be addressed
[†]School of Physics, CRANN and AMBER, Trinity College, Dublin 2, Ireland
[‡]PSE Division, KAUST, Thuwal 23955-6900, Saudi Arabia
[¶]School of Physics and CRANN/AMBER, Trinity College, Dublin 2, Ireland
[§]Current address: Johannes Gutenberg University, Institute of Physics, Spice Centre, Germany.
[‖]Current address: National Physical Laboratory, Hampton Road, TW11 OLW, United Kingdom.

DFT calculation. The coupling to the electrodes are given by $\Gamma^{\mathrm{NEGF}}_{\mathrm{L,R}}(E) = i\left(\Sigma_{\mathrm{L,R}} - \Sigma^{\dagger}_{\mathrm{L,R}}\right)$, i.e., the imaginary part of the self-energy defined as

$$\Sigma_{\mathrm{L}}(E) = (ES_{\mathrm{LD}} - V^{\dagger}_{\mathrm{LD}})\mathcal{G}_{\mathrm{L}}(E)(ES_{\mathrm{LD}} - V_{\mathrm{LD}}), \tag{2}$$

where $\mathcal{G}_{\mathrm{L}}$ is the surface Green's function of the isolated left(L) electrode and V_{LD} is the interaction between the scattering region and the electrode. All these quantities are matrices. The same can be defined for the right electrode. Finally the density of states (DOS) of the isolated left electrode can be written in terms of its Green's function as $\nu^{\mathrm{NEGF}}_{\mathrm{L}}(E) = \frac{1}{2\pi}\mathrm{Tr}\left[\mathcal{G}_{\mathrm{L}}(E) - \mathcal{G}^{\dagger}_{\mathrm{L}}(E)\right] S_{\mathrm{LD}}$. From the Green's function and couplings, the non-equilibrium charge density can be computed and by following a self-consistent procedure, for a specific applied bias, the transmission coefficients are given by $T(E) = \mathrm{Tr}\left[\Gamma_{\mathrm{L}}\mathcal{G}^{\dagger}_{\mathrm{D}}\Gamma_{\mathrm{R}}\mathcal{G}_{\mathrm{D}}\right]$. Within NEGF the electrical current between the two electrodes is

$$I = \frac{2e}{h}\int_{-\infty}^{+\infty} \mathrm{Tr}\left[\Gamma_{\mathrm{L}}\mathcal{G}^{\dagger}_{\mathrm{D}}\Gamma_{\mathrm{R}}\mathcal{G}_{\mathrm{D}}\right](f_{\mathrm{L}} - f_{\mathrm{R}})\, dE, \tag{3}$$

where $f_{\mathrm{L,R}}$ is the Fermi's distribution function of the (L,R) electrodes in its respective chemical potential $\mu_{\mathrm{L,R}}$.

Constrained Density Functional Theory and Electrostatic Model

Here we describe the CDFT method used to calculate the image charge plane used as parameter in the electrostatic classical model.[3,4] For a given distance, d, from the center of the molecule to a single metallic surface, the procedure is as follows: first, a conventional DFT calculation is performed, where no constraint is applied. This yields the total the charge density, and the amount of charge present on each fragment (one fragment being the molecule and the other fragment the metal surface). In a second step, a CDFT calculation is performed. A full electron is removed from the molecule and added to the substrate, and the

charge density is obtained. From these two sets of calculations we can evaluate the image charge plane by

$$z_0(d) = \frac{\int_{d_A}^{d_B} z\ \Delta\rho_{xy}(z;d)\ \mathrm{d}z}{\int_{d_A}^{d_B} \Delta\rho_{xy}(z;d)\ \mathrm{d}z}\ . \tag{4}$$

In other words z_0 can be interpreted as the center of gravity of the screening charge density localized on the metal surface, and in general it depends on d. Here $\Delta\rho_{xy}(z;d) = \int \mathrm{d}x\mathrm{d}y\Delta\rho(\mathbf{r};d)$ and $\Delta\rho(\mathbf{r};d)$ is the difference between the charge densities of the DFT (ground state) and the CDFT (charge transfer state) solutions for a fixed d. Note that the charge transfer between the surface and the molecule leads to the formation of a spurious charge layer on the back side of the Au slab (i.e. opposite to the surface where the molecule is placed), which is due to the finite number of atomic layers used to simulate the metal surface. In order not to consider such spurious charge while evaluating the integral in Eq. 4, the two integration limits, d_A and d_B, are chosen in the following way: 1) d_A is taken after the first two $\Delta\rho(d)$ charge oscillations on the back of the cluster, and 2) d_B is the distance at which $\Delta\rho(d)$ changes sign between the top Au layer and the molecule (i.e. it is in the vacuum). Once we have information on the image charge plane, we consider the electrostatic classical model where a point charge is interacting with two infinite flat surfaces,[5,6] given by

$$U(d) = -\frac{Q^2}{2(d/2 - z_0)}\ln 2, \tag{5}$$

where Q is a point charge located at the center of the molecule, and d is the distance between the two surfaces; z_0 is the height of the image charge plane with respect to the surface atomic layer, and is the center of gravity of the screening charge density formed on the metal surface. Since we evaluate z_0 by CDFT, our classical model is effectively parameter-free.

Scissor Operator method

For the particular case of a single molecule attached to the electrodes, first a projection of the full KS-Hamiltonian matrix and of the overlap matrix is carried out onto the atomic orbitals

associated with the molecule subspace, which we denote as $H^0_{\rm mol}$ and $S^0_{\rm mol}$ (the remaining part of $\hat{H}$ describes the electrodes). By solving the corresponding eigenvalue problem, $H^0_{\rm mol}\psi = \epsilon S^0_{\rm mol}\psi$, for this subblock we obtain the eigenvalues, $\{\epsilon_n\}_{n=1,\ldots,M}$, and eigenvectors, $\{\psi_n\}_{n=1,\ldots,M}$, where M is the number of atomic orbitals on the molecule. Subsequently, the corrections are applied to the eigenvalues, where all the occupied levels are shifted rigidly by the constant $\Sigma_{\rm o}$ while the unoccupied levels are shifted rigidly by the constant $\Sigma_{\rm u}$. We note that in principle each state can be shifted by a different amount. Using the shifted eigenvalues we can construct a transformed molecular Hamiltonian matrix, $H^{\rm SCO}_{\rm mol}$, given by

$$H^{\rm SCO}_{\rm mol} = H^0_{\rm mol} + \Sigma_{\rm o} \sum_{i_{\rm o}=1,n_{\rm o}} \psi_{i_{\rm o}}\psi^\dagger_{i_{\rm o}} + \Sigma_{\rm u} \sum_{i_{\rm u}=1,n_{\rm u}} \psi_{i_{\rm u}}\psi^\dagger_{i_{\rm u}}, \tag{6}$$

where the first sum runs over the $n_{\rm o}$ occupied orbitals, and the second one runs over the $n_{\rm u}$ empty states. In the full Hamiltonian matrix we then replace the subblock $H^0_{\rm mol}$ with $H^{\rm SCO}_{\rm mol}$.[5–9] The SCO procedure can be applied self-consistently, although in this work we apply it non-selfconsistently to the converged DFT Hamiltonian.

The correction applied to the frontier energy levels of a molecule in a junction has two contributions. First we need to correct for the fact that the gas-phase LDA HOMO-LUMO gap ($E^{\rm gap}_{\rm LDA}$) is too small when compared to the difference between $I_{\rm P}$ and $E_{\rm A}$. Secondly, the renormalization of the energy levels (Eq. 5), when the molecule is brought close to metal surfaces needs to be added to the $I_{\rm P}$ and $E_{\rm A}$ levels. Hence, for the molecule attached to two metallic surfaces forming a molecular junction, we approximate the overall corrections for the molecular levels below $E_{\rm F}$ by

$$\Sigma_{\rm o}(d) = -[I_{\rm P} + \epsilon_{\rm HOMO}] + U(d) \tag{7}$$

and similarly for the levels above $E_{\rm F}$ as

$$\Sigma_{\rm u}(d) = -[E_{\rm A} + \epsilon_{\rm LUMO}] - U(d); \tag{8}$$

where $\epsilon_{\mathrm{HOMO/LUMO}}$ are the gas-phase KS eigenvalues.

Model Hamiltonian and master equation for electronic transport

The steady-state current are computed via the master equation formalism. Within the $\mathscr{T}$-matrix[10–13] approach we evaluate the diagonal terms of the reduced density matrix[13,14] and the steady-state occupation probabilities are obtained as

$$\dot{\rho}_m^q(t) = \sum_{\alpha;n\neq m,q'} \left(\Gamma_\alpha^{nm;q'q}\rho_n^{q'} - \Gamma_\alpha^{mn;qq'}\rho_m^q\right) + \sum_{\alpha\alpha';n,q'} \left(\Gamma_{\alpha\alpha'}^{nm;q'q}\rho_n^{q'} - \Gamma_{\alpha\alpha'}^{mn;qq'}\rho_m^q\right) + \frac{1}{\tau}\left(\rho_m^q - \rho_{\mathrm{eq}}^q \sum_{q'}\rho_n^{q'}\right), \tag{9}$$

where ρ_m^q is the occupation of the state $|m,q\rangle$. To lowest order in the tunnelling Hamiltonian, $\hat{H}_{\mathrm{T}}$, one describes the *sequential-tunnelling* processes where one electron is transferred from one electrode to the molecule and vice-versa. The transition rates, $\Gamma_\alpha^{mn,qq'}$, for electrons to tunnel between the molecule and the electrode α when the molecule makes a transition from the state $|m;q\rangle$ with total energy E_{mq} to the state $|n;q'\rangle$ of energy $E_{nq'}$ are given by[13,15]

$$\Gamma_\alpha^{mn,qq'} = \frac{\Gamma_\alpha}{\hbar}\sum_{i\sigma}\left\{f(E_{mq}-E_{nq'}-\mu_\alpha)|A_{nm}^{i\sigma}|^2|F_{q'q}|^2 + \left[1-f(E_{nq'}-E_{mq}-\mu_\alpha)\right]|A_{mn}^{i\sigma}|^2|F_{qq'}|^2\right\}, \tag{10}$$

where $m \to n$ and $q \to q'$ represent changes on the number of electrons and excited vibrons, respectively. $\Gamma_\alpha = 2\pi\gamma_\alpha^2\nu_\alpha$ are the bare electronic couplings to the electrodes, ν_α is the density of states and γ_α is the momentum independent hopping parameter. Moreover, $A_{n'n''}^{i\sigma} = \langle n'|\, c_{i\sigma}\,|n''\rangle = \delta_{n',n''+1}$ is the matrix element of the annihilation operator for the single-particle state i with spin σ and $F_{q'q} = \langle q'|\, e^{-\lambda(\hat{b}^\dagger-\hat{b})}\,|q\rangle$ are the Franck-Condon matrix elements.[14,16] These processes are dominant as long as the conducting energy level is within the bias window. However, if the level is outside the bias window, the sequential tunnelling decreases exponentially and higher order processes will dominate.

To the next-to leading-order of the $\mathscr{T}$-matrix expansion, *cotunnelling* processes dominate

(second term of Eq. 9) and the transition rates are given by[11,13,17–19]

$$\Gamma_{\alpha\alpha'}^{nn';qq'} = \frac{\Gamma_\alpha \Gamma_{\alpha'}}{2\pi\hbar} \sum_{i''\sigma''} \sum_{i'\sigma'} \int dE \left| \sum_{n'',q''} \left(\frac{A_{n'n''}^{i''\sigma''} A_{nn''}^{i'\sigma'*} F_{q'q''} F_{qq''}^*}{E + E_{nq} - E_{n''q''} + i\eta} + \frac{A_{n''n'}^{i''\sigma''*} A_{n''n}^{i'\sigma'} F_{q''q'}^* F_{q''q}}{-E + E_{n'q'} - E_{n''q''} + i\eta} \right) \right|^2 \times f(E - \mu_\alpha)\big[1 - f(E + E_{nq} - E_{n'q'} - \mu_{\alpha'})\big]. \tag{11}$$

$\Gamma_{\alpha\alpha'}^{nn';qq'}$ describes the transition rates to transfer coherently (tunnelling) one electron from the electrode α while the molecule is in the state $|n;q\rangle$ to the electrode α' and leaving the molecule in the state $|n';q'\rangle$. The occupation of the molecule changes just virtually in the intermediate state, i.e., the number of electrons in the molecule is the same during cotunnelling processes. We disregard tunnelling processes changing the number of electrons in the molecule by ± 2. This is achieved by constructing a general final state as $|j'\rangle\,|n'\rangle = \hat{d}_{\alpha'\mathbf{k}'}^\dagger \hat{d}_{\alpha\mathbf{k}}\,|j\rangle\,|n'\rangle$, with $\alpha \neq \alpha'$. Note that Eq. (11) can not be directly computed due to the second order poles. To circumvent this, we apply a regularization scheme as presented in Ref.[14].

By solving Eq. (9) with the time derivatives set to zero and the normalization condition $\sum_i \rho_i = 1$ one obtains the steady-state current through the left electrode as[13,14]

$$I^{\mathrm{L}} = -e \sum_{nm;qq'} (N_n - N_m)\, \Gamma_{\mathrm{L}}^{nm;q'q} \rho_{m;q} - e \sum_{nm;q'q} \left(\Gamma_{\mathrm{LR}}^{nm;q'q} - \Gamma_{\mathrm{RL}}^{nm;q'q} \right) \rho_{m;q}, \tag{12}$$

where N_n is the number of electrons in state $|n;q\rangle$. In our model, we map the problem in an orthogonal basis set and we consider only the two single-particle states relevant to the problem, i.e., they represent the frontier highest occupied molecular orbital (HOMO) and the lowest unoccupied molecular orbital (LUMO). The states are considered spin-degenerated so that the contributions of each spin are cast out into a spin factor constant.[14] For simplicity, we do not allow a second electron in the molecule, i.e., $\mathcal{U} \to \infty$. Therefore, the states used to construct the basis set for the reduced density matrix are $|0;q\rangle$, $|1,0;q\rangle$ and $|0,1;q\rangle$, i.e., empty molecule, an electron in the HOMO and an electron in the LUMO, respectively, for

q number of vibrons.

Fig. S1 shows the total current and the sequential tunnelling contributions. The cotunnelling current adds minor features in the current-voltage profile, beind dominant in the region of small bias. The oscillatory feature at voltages corresponding to the position of the energy levels is due to the fact that the cotunnelling current changes sign,[16] as also shown in Fig. 4 of the main text.

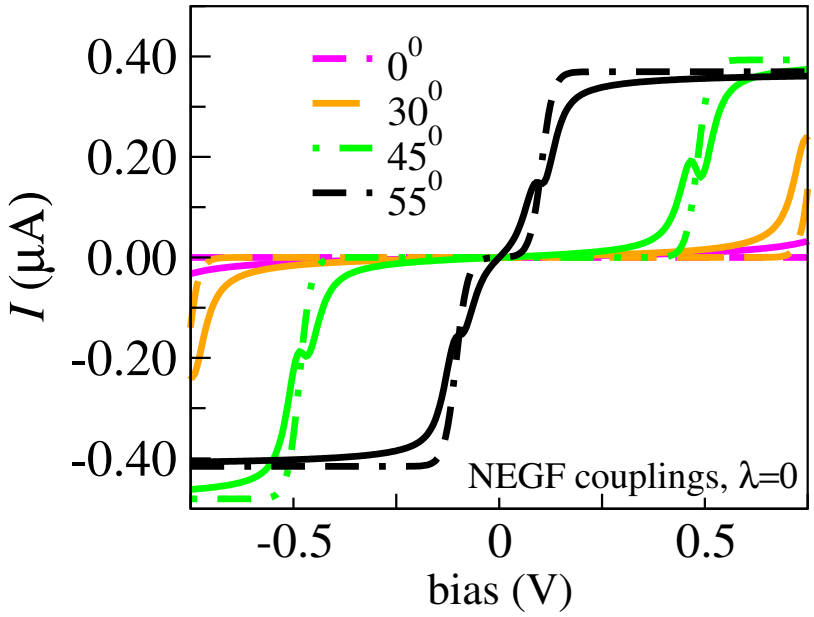

Figure S1: Transport properties of several thiol-terminated junctions for different binding angle, θ, as obtained from the ME: Total current (solid lines) and sequential tunnelling contribution (dashed-dotted lines) as a function of bias at a temperature $\Theta = 80$ K. The position of the energy levels and the electronic couplings are given by Fig. 3 and Table 1 in the main text, respectively.

Extracting electronic couplings from DFT-NEGF calculations

The energy level alignment as a function of the electrode separation is determined (see computational methods in the main text) and a scissor operator approach is used to shift the energy levels to the corrected positions.[3,4] Subsequently, we perform the transport calculations within NEGF and obtain the transmission coefficients with the corrected energy levels positions. The electronic couplings are extracted by fitting a Lorentzian curve[20] to

the transmission coefficients as

$$T(E) = \sum_i \frac{\Gamma_{\mathrm{L}i}\Gamma_{\mathrm{R}i}}{\left(E - E_i\right)^2 + \frac{1}{4}\left(\Gamma_i\right)^2}, \tag{13}$$

where $\Gamma_i = \Gamma_{\mathrm{L}i} + \Gamma_{\mathrm{R}i}$ for $i = \mathrm{HOMO}, \mathrm{LUMO}$ levels.

In order to make the connection between the electronic couplings obtained with NEGF, $\Gamma_{\mathrm{L,R}}^{\mathrm{NEGF}}(E)$, and the ones defined within ME, Γ_α, we first assume that the scattering region (within ME) is given just by the molecule and that its energy levels are non-degenerated and well separated in energy. Therefore, the interaction $V_{\mathrm{L,R}}$ between the scattering region and the electrode is given, for a single-particle level, by the momentum independent hopping parameter $\gamma_{\mathrm{L,R}}$. Then, the self-energy given in Eq. (2) becomes $\Sigma_{\mathrm{L,R}}(E) = \pi\gamma_{\mathrm{L,R}}^2\nu_{\mathrm{L,R}}^{\mathrm{NEGF}}(E)$. If we further assume the wide-band approximation, i.e., the density of states is energy independent which is a good approximation for metallic electrodes, we obtain

$$\Gamma_{\mathrm{L,R}}^{\mathrm{NEGF}} = 2\pi\gamma_{\mathrm{L,R}}^2\nu_{\mathrm{L,R}}^{\mathrm{NEGF}} \approx 2\pi\gamma_{\mathrm{L,R}}^2\nu_{\mathrm{L,R}} \equiv \Gamma_{\mathrm{L,R}}. \tag{14}$$

We note that, for a metallic surface, DFT-LDA generally yields satisfactory results for $\nu_{\mathrm{L,R}}$. Fig. S2 shows the non-self-consistent transmission coefficients through the KS-HOMO level for different values of applied bias. By evaluating Eq. 13 we extract the electronic couplings and we observe a reduction of about 20 % for 2 V when compared to 0 V. This explains the reduction of the current as we increase the bias voltage, see black-dashed line of Fig. 4. Moreover, the extracted couplings for the non-self-consistent transmission at 0 V ($\Gamma_{\mathrm{L,R}} \sim 0.01$ eV) are larger than the ones for the self-consistent case shown in Tab. 1 ($\Gamma_{\mathrm{L,R}} \sim 0.006$ eV). This explains, in Fig. 5 of the main text, why the non-self-consistent current (black-dashed line) is larger than the current obtained with the master equation (blue-solid line).

We have performed transport calculations for the flat and tip electrodes where we change symmetrically the distance between the linking group and the gold atom. From this we extract the electronic couplings for the HOMO level as a function of the S-Au distance. Fig.

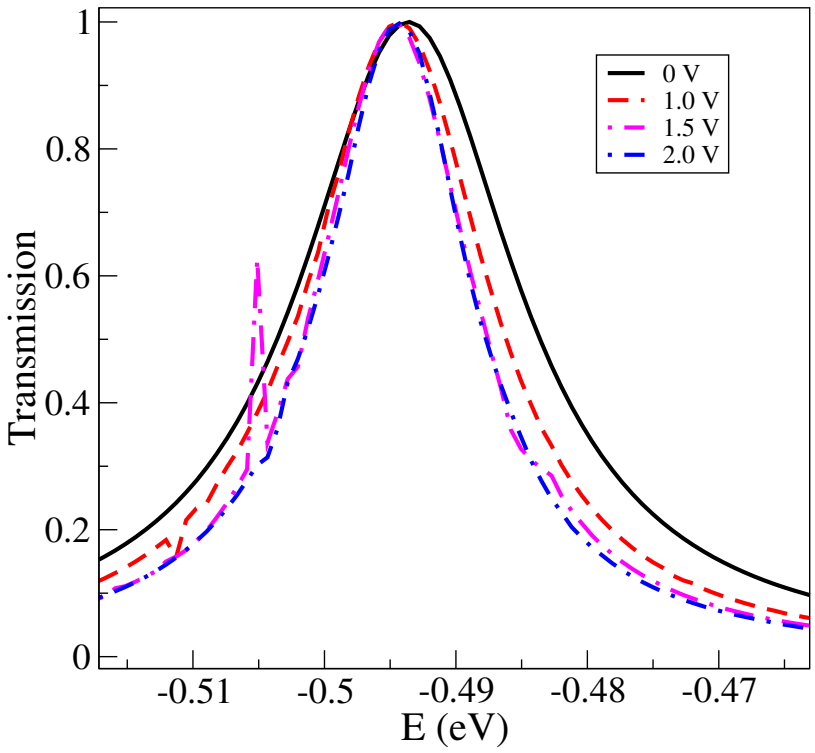

Figure S2: Non-self-consistent transport calculation for $\theta = 0^0$. Transmission as a function energy for different values of bias voltage. The resonant peak corresponds to the KS-HOMO level. The different width of the peaks show that the electronic couplings are reduced when the bias voltage increases. For 0 V, $\Gamma = 0.01$ eV whereas for 2 V, $\Gamma = 0.008$ eV.

S3(a)-(b) shows the transmission coefficients for the equilibrium position (d_{S-Au}=2 Å) and compare to the case where we increase the bond length by 0.5 Åand 1.5 Å. Fig. S3(c)-(d) show the respective electronic couplings. In Fig. S3(d) we also show the electronic coupling extracted for Fig 1(d) in the main text.

Fig. S4 we show how the current depends on the number of vibrons (q_{max}), the electron-vibron coupling strength (λ) and on the vibron relaxation time τ. We have considered $q_{max} \leq 150$ for which above this value numerical problems arise since the transition rates matrix becomes bad-ranked. Fig. S4(a)-(b) show the current versus bias for several values of q_{max} and λ. For values of $\lambda \leq 1.5$ the excitations do not lead to the linear increase of the current after the onset. Nevertheless, for $\lambda = 2$ and $q_{max} \geq 100$ is already visible the increase in the current due to vibration excitations. In particular, for $q_{max} \geq 120$ the current increases rapidly due to avalanche effects as discussed by Koch et. al (PRB 74, 205438,

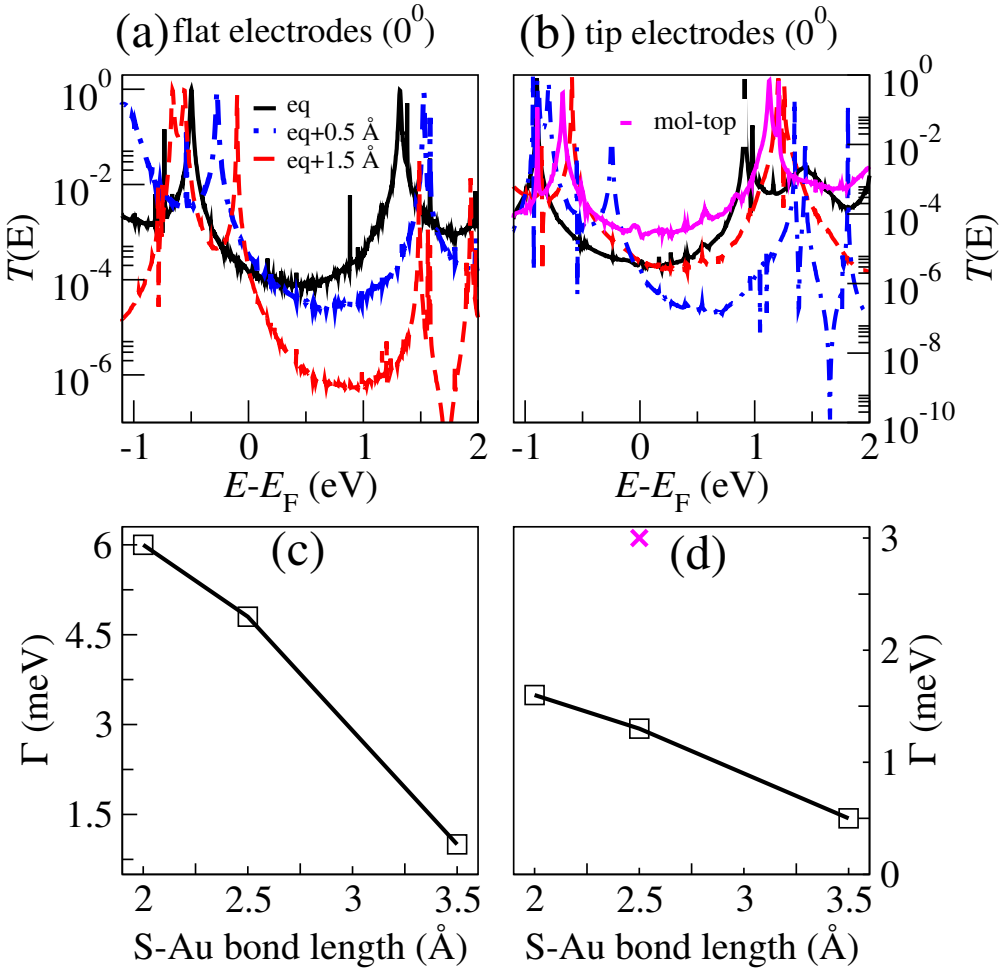

Figure S3: Transmission coefficients for flat electrodes (a) and tip electrodes (b) for different distances between the linking SH group and the gold atoms. (c) and (d) show the electronic couplings for the HOMO level as a function of the S-Au distance where the equilibrium distance is 2 Å. The purple data point in (d) shows the electronic coupling for the HOMO when the molecule is placed on top of the two tips, as shown in Fig. 1(d) in the main text.

2006). When we include vibron relaxation [Fig. S4(c)] we observe a sensitive dependence on the values of τ when considering $q_{max} = 150$. Although we treat the relaxation time for vibrations as a parameter by setting it to 1 ps, this is the order of magnitude for vibration relaxation time in closely related systems.[21,22]

In Fig. S5 we show the wavefunction plots for the frontier molecular levels HOMO and LUMO for the isolated ZnTPPdT(thiol) molecule.

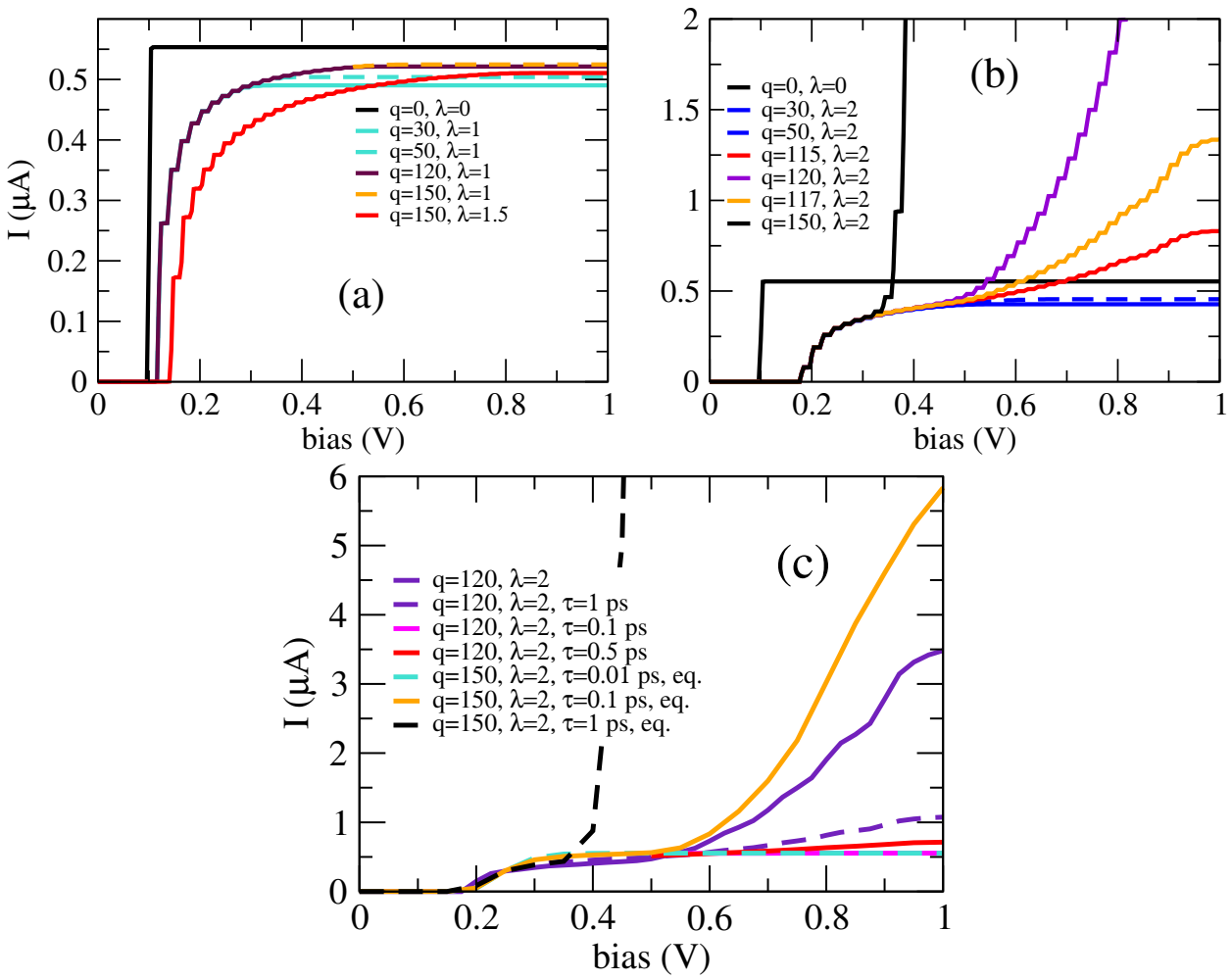

Figure S4: Sequential tunneling current versus bias for a single-level model with vibrations. (a)-(b) Several values of q_{max} and λ without vibron dissipation, i.e., $\tau = 0$. (c) Comparison when vibron relaxation is allowed. Other parameters: $\Gamma_{\mathrm{L(R)}}$=6 (5.5) meV. $k_{\mathrm{B}}\Theta$=0.34 meV, $\hbar\omega_p$= 10 meV.

References

(1) Rocha, A. R.; García-Suárez, V. M.; Bailey, S.; Lambert, C.; Ferrer, J.; Sanvito, S. *Phys. Rev. B* **2006**, *73*, 85414–85435.

(2) Rungger, I.; Sanvito, S. *Phys. Rev. B* **2008**, *78*, 035407–035420.

(3) Souza, A. M.; Rungger, I.; Pemmaraju, C. D.; Schwingenschloegl, U.; Sanvito, S. *Phys. Rev. B* **2013**, *88*, 165112–165121.

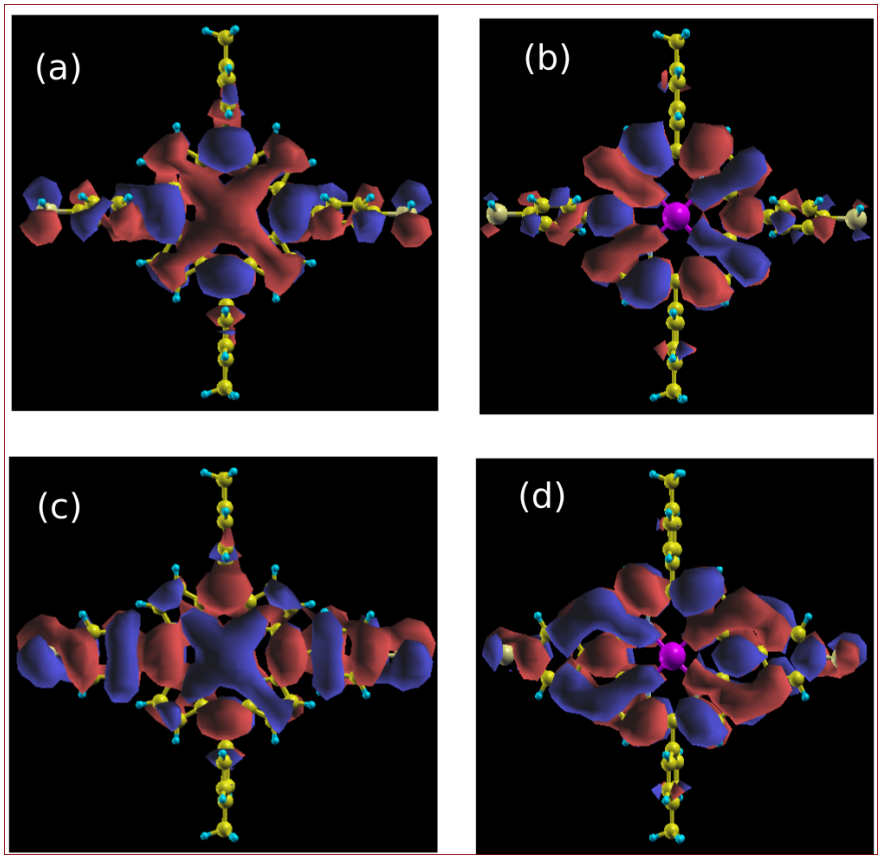

Figure S5: Isosurfaces for the frontier energy levels of the ZnTPPdT(thiol) molecule. (a)-(b) are the KS-HOMO and KS-LUMO for the relaxed structure. (c)-(d) are the same for the molecule where we forced the side phenil rings connected to the sulfur atoms to be parallel to the main porphyrin ring. Isosurface equal 0.02 $e/\text{Å}^3$.

(4) Souza, A. M.; Rungger, I.; Pontes, R. B.; Rocha, A. R.; da Silva, A. J. R.; Schwingenschlöegl, U.; Sanvito, S. *Nanoscale* **2014**, *6*, 14495–14507.

(5) Quek, S. Y.; Venkataraman, L.; Choi, H. J.; Louie, S. G.; Hybertsen, M. S.; Neaton, J. B. *Nano Lett.* **2007**, *7*, 3477–3482.

(6) García-Suárez, V. M.; Lambert, C. J. *New J. Phys.* **2011**, *13*, 53026.

(7) Quek, S. Y.; Choi, H. J.; Louie, S. G.; Neaton, J. B. **2011**, *5*, 551–557.

(8) Mowbray, D. J.; Jones, G.; Thygesen, K. S. *J. Chem. Phys.* **2008**, *128*, 111103.

(9) Abad, E.; Ortega, J.; Dappe, Y. J.; Flores, F. *Appl. Phys. A* **2008**, *95*, 119–124.

(10) Timm, C. *Phys. Rev. B* **2008**, *77*, 195416–195429.

(11) Begemann, G.; Koller, S.; Grifoni, M.; Paaske, J. *Phys. Rev. B* **2010**, *82*, 045316–045327.

(12) Koller, S.; Grifoni, M.; Leijnse, M.; Wegewijs, M. R. *Phys. Rev. B* **2012**, *82*, 235307–235334.

(13) Elste, F.; Timm, C. *Phys. Rev. B* **2007**, *75*, 195341–195349.

(14) Koch, J.; von Oppen, F.; Oreg, Y.; Sela, E. *Phys. Rev. B* **2004**, *70*, 195107–195129.

(15) Muralidharan, B.; Ghosh, A. W.; Pati, S. K.; Datta, S. *IEEE Trans. Nanotechnol.* **2007**, *6*, 536–544.

(16) Koch, J.; von Oppen, F.; Andreev, A. V. *Phys. Rev. B* **2006**, *74*, 205438–205457.

(17) Hansen, T.; Mujica, V.; Ratner, M. A. *Nano Lett.* **2008**, *8*, 3525–3531.

(18) Pedersen, J. N.; Wacker, A. *Phys. E Low-dimensional Syst. Nanostructures* **2010**, *42*, 595–599.

(19) Turek, M.; Matveev, K. *Phys. Rev. B* **2002**, *65*, 115332–1153341.

(20) Datta, S. *Quantum Transport: Atom to Transistor*; Cambridge University Press, Cambridge, 2005.

(21) Helbing, J.; et. al., *Biophysical Journal* **2004**, *87*, 1881–1891.

(22) Lian, T.; et. al., *J. Phys. Chem.* **1994**, *98*, 11648–11656.